Coastal Engineering in Japan

ISSN: 0578-5634 (Print) (Online) Journal homepage: https://www.tandfonline.com/loi/tcej19

Statistical Variability of Sea State Parameters as a Function of Wave Spectrum

Yoshimi Goda

To cite this article: Yoshimi Goda (1988) Statistical Variability of Sea State Parameters as a Function of Wave Spectrum, Coastal Engineering in Japan, 31:1, 39-52, DOI: 10.1080/05785634.1988.11924482

To link to this article: https://doi.org/10.1080/05785634.1988.11924482

Published online: 11 Jan 2018.

Coastal Engineering in Japan, Vol. 31, No. 1, 1988

STATISTICAL VARIABILITY OF SEA STATE PARAMETERS AS A FUNCTION OF WAVE SPECTRUM [1]

Yoshimi Goda [2]

ABSTRACT

Statistical properties of zero-upcrossing wave heights and periods are examined with a large number of linearly simulated wave profiles for sixteen frequency spectra of the Wallops and JONSWAP types. The means and standard deviations of various parameters are presented as the reference to the statistical studies of sea waves.

I. INTRODUCTION

The random nature of sea waves has attracted the attention of many scientists and engineers. Several important statistical theories for sea state parameters have been derived, a great deal of field wave records have been taken and analyzed at various waters around the world, and a number of simulation studies have been undertaken to fill the gap of our knowledge on wave statistics. As the results of such efforts, we know for example that the zero-upcrossing or zero-downcrossing wave heights approximately follow the Rayleigh distribution even for waves with a broad bandwidth spectrum.

Nevertheless there are still many unsolved problems on wave statistics. One example is the relationships between various period parameters such as $T_{H1/3}$ and $\bar{T}$ which are governed by the joint distribution between wave heights and periods. Theories by Longuet-Higgins (1975 and 1983) and Cavanié et al. (1976) give us powerful tools to look into the structure of joint distribution, but they cannot truly represent the actual distribution of field waves (e.g. Goda 1978). Statistical variability of sea state parameters is another unanswered question. An early theory by Tucker (1957) makes it possible to estimate the coefficient of variation of σ_η for a given spectrum, but not those of wave height parameters.

Difficulty in theoretical development for wave statistics originates from the artifice of the zero-crossing definition. Search for the highest and lowest elevations among many maxima and minima between two successive zero-crossing points is not easily adaptable for mathematical formulation, especially for broad bandwidth spectra. This difficulty can be overcome by numerical simulation techniques. Even though a simulation study cannot produce the solid basis of wave statistics as the theory does, the reliability of the data obtained by a simulation study increases as the number of wave profile data is increased.

The present paper examines the statistical properties of the wave height and period parameters by means of the numerical, linear simulation technique for various single-peaked wave spectra. The mean values of sea state parameters and their mutual ratios are given as a function of spectral shape parameter. The standard deviations of these parameters are also analyzed for various spectral forms.

[1] This paper has been presented at the IAHR Seminar of Maritime Hydraulics Section on Wave Analysis and Generation in Laboratory Basins, 1–4 September 1987 (Goda 1987), and is republished here in a revised form under the permission of the National Research Council of Canada.

[2] Dr. Eng., Port and Harbour Research Institute, Ministry of Transport, Nagase, Yokosuka. Presently, Professor of Civil Engineering, Yokohama National University, Japan.

II. WAVE SPECTRA AND SIMULATION METHOD

Two standard spectral functions are chosen for the present study. They are the Wallops-type spectrum (Huang et al., 1981) and the JONSWAP-type spectrum (Hasselmann et al., 1973) of the following:

Wallops-type Spectrum:

$$S(f) = \beta_W H_{1/3}^2 T_p^{1-m} f^{-m} \exp\left[-\frac{m}{4}(T_p f)^{-4}\right]. \tag{1}$$

JONSWAP-type Spectrum:

$$S(f) = \beta_J H_{1/3}^2 T_p^{-4} f^{-5} \exp\left[-\frac{5}{4}(T_p f)^{-4}\right] \gamma^{\exp[-(T_p f-1)^2/2\delta^2]}, \tag{2}$$

where,

$$\delta = \begin{cases} \delta_a: & f \le f_p, \\ \delta_b: & f > f_p, \end{cases} \quad (\delta_a = 0.07, \quad \delta_b = 0.09).$$

The notations are consistent with "IHAR List of Sea State Parameters," except for the omission of the subscript "d" or "u", which stands for the downcrossing or upcrossing definition, respectively. The omission is based on the confirmation by numerical simulations the linear wave profiles yield the statistically same values of sea state parameters (Goda, 1986). The constants β_W and β_J are later determined by the relationship between $H_{1/3}$ and the zeroth moment of spectrum. The spectral peak period T_p is also related to $T_{H1/3}$ or $\bar{T}$ as shown later.

The spectral shape parameter m of the Wallops-type spectrum is varied between 3 and 20 to simulate various wave conditions from shallow water waves to long-travelled swell. The peak enhancement factor γ of the JONSWAP-type spectrum is also varied between 1 and 20.

Simulation of wave profiles is made using the Inverse Fast Fourier Transform method. The Gaussian random variable generating algorithm[3] is used to determine the amplitudes of Fourier components on the basis of spectral information. The simulation condition is as follows:

Frequency range	:	$f/f_p = 0.6 - 6.0$.
Sampling time interval	:	$\Delta t = T_p/12$.
Number of data points	:	$N = 4096 \quad (= 341.3 T_p)$.

Two runs of simulation each with one thousand different wave profiles are carried out for each wave spectrum in order to insure the reliability of the results of simulation data. Simulated wave profiles are analyzed by the standard zero-upcrossing method to yield various height and period parameters. For each run with 1000 wave profiles, the means and standard deviations of various parameters are calculated and the data of two runs are averaged to yield the final results; the differences between them are within the range of statistical errors. For the analysis of statistical variability, short records of wave profiles with the data points of 512, 1024, and 2048 are prepared by adopting the initial portion of the full record with 4096 data points. These short records are analyzed similarly, and the tendency of decrease of the standard deviation of various parameters with the increase of the number of waves are examined.

[3] A test has proven that the algorithm employed here does not exhibit any indication of violating randomness even after 10 million cycles.

III. MEAN VALUES OF HEIGHT AND PERIOD PARAMETERS

Tables 1 and 2 list the results of the mean values of various height and period parameters. The notations for wave periods are abbreviated for the sake of simplicity. The following is the comments on the results of Tables 1 and 2. (Some of the data show slight irregularities in the variation with respect to spectral shapes, but it is probably due to statistical errors.)

Maximum Height and Elevation

The theory of the Rayleigh distribution predicts the following mean value for H_{max}, which is based on the assumption of H_{max} being twice the maximum surface elevation η_{max}:

$$E[x_{max}] = \frac{1}{a}(\ln N_0)^{1/2} + \frac{\zeta}{2a(\ln N_0)^{1/2}} - \frac{\pi^2 + \zeta^2}{48a(\ln N_0)^{3/2}} + \cdots, \tag{3}$$

where,

$$x_{max} = H_{max}/H_*,$$
$$a = \begin{cases} 1/2\sqrt{2} & : \quad H_* = m_0^{1/2} = \sigma_\eta, \\ 1.416 & : \quad H_* = H_{1/3}, \end{cases} \tag{4}$$
$$\zeta = 0.5772 \cdots : \text{Euler's constant},$$

and N_0 denotes the number of zero-upcrossing or zero-downcrossing waves per record.

The theoretical value of the maximum elevation η_{max} is one-half the value given by Eq. (3). In both Tables 1 and 2, the parameters related with η_{max} and H_{max} are listed as the ratio of the observed value to the theoretical prediction by Eq. (3). The observed value of η_{max} is the simulation refers to the highest elevation in a continuous wave profile, and it does not necessarily belong to the highest wave in the same data; some η_{max} is accompanied by a quite shallow wave trough and the resultant height is not the largest in the wave group.

It is interesting to note that η_{max}/σ_η is very close to the theoretical prediction, but H_{max}/σ_η indicates appreciable deviation from the theory. As a result, the ratio η_{max}/H_{max} remains above 0.5 even though wave profiles are linearly simulated ones. This fact can be explained in such a way that the highest wave crest in a wave train is not necessarily followed by the lowest trough in the wave train. The height of the wave trough following the highest crest is mostly less than the height of the latter. Therefore, H_{max} is less than $2\eta_{max}$ on the average.

Another point of interest is the fact that the difference between the observation and theory of η_{max}/σ_η rather increases as the spectral peak becomes sharp. It is due to the tendency that the correlation between successive wave heights increases as the spectral peak becomes sharp. A strong correlation means that a set of wave height data within a continuous record does not constitute a data of randomly sampled wave heights, and this violates the basic assumption of independent data in the theory of Rayleigh distribution by Longuet-Higgins (1952).

Wave Height Parameters

All the parameters $H_{1/10}$, $H_{1/3}$, $\bar{H}$ and σ_H exhibit the values less than the predictions by the Rayleigh distribution in terms of σ_η. The deviations of the height parameters from the Rayleigh distribution gradually decreases as the spectral peak becomes sharp. The commonly observed relation of $H_{1/3} = 3.8\sigma_\eta$ in field wave records instead of $H_{1/3} = 4.004\sigma_\eta$ is again confirmed in the present simulation. It should be mentioned here however that the value of the ratio $H_{1/3}/\sigma_\eta$ may exceed 4.0 in shallow water because of wave nonlinearity effect, as pointed out by the author (1983b).

Table 1 Mean values of statistical parameters of Wallops-type spectrum ($f_{max} = 6f_p$)

Parameter	m=3	m=4	m=5	m=6	m=8	m=10	m=14	m=20	Rayleigh
$\{\eta_{max}/\sigma_\eta\}^*$	0.992*	0.998*	1.000*	1.000*	1.000*	0.998*	0.992*	0.981*	1.000*
$\{H_{max}/\sigma_\eta\}^*$	0.893*	0.911*	0.925*	0.935*	0.949*	0.956*	0.962*	0.961*	1.000*
η_{max}/H_{max}	0.560	0.551	0.544	0.538	0.528	0.522	0.515	0.511	0.500
$H_{1/10}/\sigma_\eta$	4.658	4.734	4.781	4.818	4.877	4.912	4.971	5.007	5.090
$H_{1/3}/\sigma_\eta$	3.736	3.800	3.830	3.848	3.874	3.895	3.924	3.948	4.004
$\bar{H}/\sigma_\eta$	2.359	2.412	2.448	2.470	2.488	2.495	2.501	2.504	2.507
σ_H/σ_η	1.201	1.218	1.218	1.217	1.221	1.230	1.246	1.261	1.309
$\{H_{max}/H_{1/3}\}^*$	0.958*	0.961*	0.967*	0.974*	0.981*	0.984*	0.983*	0.976*	1.000*
$H_{1/10}/H_{1/3}$	1.247	1.246	1.248	1.251	1.259	1.263	1.267	1.268	1.271
$\bar{H}/H_{1/3}$	0.631	0.635	0.639	0.642	0.642	0.641	0.638	0.635	0.626
$H_{1/3}/\bar{H}$	1.584	1.576	1.565	1.558	1.557	1.561	1.569	1.577	1.597
$T_{H1/10}/T_p$	0.824	0.866	0.889	0.899	0.915	0.927	0.943	0.959	1.000
$T_{H1/3}/T_p$	0.782	0.848	0.883	0.902	0.923	0.934	0.947	0.960	1.000
$\bar{T}/T_p$	0.579	0.671	0.740	0.791	0.851	0.885	0.921	0.946	1.000
σ_T/T_p	0.252	0.255	0.246	0.234	0.213	0.198	0.176	0.155	0.000
$T_{H,max}/T_{H1/3}$	1.066	1.009	0.987	0.980	0.980	0.985	0.990	0.994	1.000
$T_{H1/10}/T_{H1/3}$	1.055	1.021	1.004	0.997	0.992	0.993	0.996	0.998	1.000
$T_{H1/3}/\bar{T}$	1.350	1.265	1.192	1.142	1.084	1.055	1.028	1.015	1.000
r_{HT}	0.711	0.663	0.595	0.525	0.413	0.336	0.242	0.173	0.000
r_{HH}	0.172	0.241	0.293	0.333	0.395	0.445	0.525	0.611	1.000

Note: The figures superscribed with * refer to the ratio of the observed value to the theoretical prediction by the Rayleigh distribution.

Table 2 Mean values of statistical parameters of JONSWAP-type spectrum ($f_{max} = 6f_p$)

Parameter	$\gamma = 1$	$\gamma = 1.5$	$\gamma = 2$	$\gamma = 3.3$	$\gamma = 5$	$\gamma = 7$	$\gamma = 10$	$\gamma = 14$	$\gamma = 20$
$\{\eta_{max}/\sigma_\eta\}^*$	1.000*	1.000*	0.995*	0.996*	0.993*	0.983*	0.981*	0.969*	0.964*
$\{H_{max}/\sigma_\eta\}^*$	0.925*	0.929*	0.927*	0.935*	0.938*	0.934*	0.937*	0.931*	0.930*
η_{max}/H_{max}	0.544	0.541	0.539	0.534	0.530	0.528	0.527	0.521	0.518
$H_{1/10}/\sigma_\eta$	4.781	4.801	4.813	4.849	4.877	4.894	4.921	4.938	4.959
$H_{1/3}/\sigma_\eta$	3.830	3.842	3.850	3.866	3.884	3.895	3.910	3.920	3.933
$\bar{H}/\sigma_\eta$	2.448	2.452	2.455	2.461	2.469	2.476	2.482	2.490	2.495
σ_H/σ_η	1.219	1.226	1.231	1.242	1.249	1.253	1.259	1.261	1.266
$\{H_{max}/H_{1/3}\}^*$	0.967*	0.968*	0.965*	0.969*	0.968*	0.962*	0.962*	0.954*	0.950*
$H_{1/10}/H_{1/3}$	1.248	1.250	1.250	1.253	1.256	1.256	1.259	1.260	1.261
$\bar{H}/H_{1/3}$	0.639	0.638	0.638	0.636	0.636	0.636	0.635	0.635	0.635
$H_{1/3}/\bar{H}$	1.565	1.567	1.569	1.573	1.574	1.573	1.576	1.575	1.577
$T_{H1/10}/T_p$	0.886	0.891	0.914	0.933	0.946	0.954	0.962	0.968	0.973
$T_{H1/3}/T_p$	0.883	0.901	0.914	0.934	0.948	0.957	0.965	0.970	0.975
$\bar{T}/T_p$	0.740	0.760	0.775	0.804	0.830	0.851	0.873	0.892	0.911
$3T/T_p$	0.246	0.247	0.247	0.244	0.238	0.238	0.220	0.208	0.195
$T_{H,max}/T_{H1/3}$	0.987	0.989	0.989	0.987	0.987	0.987	0.988	0.988	0.989
$T_{H1/10}/T_{H1/3}$	1.004	1.003	1.001	0.997	0.997	0.997	0.997	0.998	0.998
$T_{H1/3}/\bar{T}$	1.192	1.186	1.180	1.162	1.143	1.125	1.106	1.088	1.071
r_{HT}	0.595	0.596	0.596	0.587	0.571	0.553	0.527	0.497	0.459
r_{HH}	0.293	0.334	0.369	0.446	0.509	0.561	0.620	0.671	0.719

Note: The figures superscribed with * refer to the ratio of the observed values to the theoretical prediction by the Rayleigh distribution.

Ratio between Wave Height Parameters

The ratios $H_{1/10}/H_{1/3}$ and $H_{1/3}/\bar{H}$ take the values less than the predictions by the Rayleigh distribution. This tendency suggests that the distribution of wave heights is slightly narrower than the Rayleighan. The effect of spectral shape on the wave height distribution is not as large as predicted by Tayfun (1983).

Wave Period Parameter

The period parameters $T_{H1/10}$, $T_{H1/3}$, and $\bar{T}$ uniformly approach to T_p as the spectral peak becomes sharp, while σ_T decreases gradually. It is noted that the ratio $\bar{T}/T_p$ listed in Tables 1 and 2 for small values of m could have slightly been affected by the cut of high frequency range over $f_{max} = 6 f_p$ which is used in the present simulation.

Ratio between Wave Period Parameters

The wave periods $T_{H,max}$, $T_{H1/10}$, and $T_{H1/3}$ take almost the same value on the average, except for the case where the correlation coefficient r_{HT} exceeds about 0.6. On the other hand, the ratio $T_{H1/3}/\bar{T}$ varies from 1.35 to 1.02 for m = 3 to 20 and from 1.19 to 1.09 for γ=1 to 20. When a wave registration is made with quite high frequency resolution ($f_{max} \gg f_p$), there is a possibility that the mean wave period becomes quite short especially for wave with broad spectral peaks. In such a case, the ratio $T_{H1/3}/\bar{T}$ will exceed the value listed in Tables 1 and 2.

Correlation Coefficients

The correlation coefficient r_{HH} between successive wave heights increases as the spectral peak becomes sharp, while the correlation coefficient r_{HT} between wave heights and periods decreases. The latter decrease is rather slow in the case of the JONSWAP-type spectrum, probably owing to the presence of the high frequency tail.

IV. STANDARD FORM OF FREQUENCY SPECTRUM

With the results of Tables 1 and 2, it is possible to formulate the standard form of frequency spectrum in terms of the sea state parameters defined by the zero-crossing method. The constants β_W and β_J are determined with the data of $H_{1/3}/\sigma_\eta$ as the function of m or γ by empirical application of the regression analysis. The data of $T_{H1/3}/T_p$ and $\bar{T}/T_p$ are also subjected to the regression analysis in order to fix the position of spectral peak in terms of zero-upcrossing or zero-downcrossing wave periods. The following is the result of the formulation:

FORMULA I: Modified Wallops-type of Eq. (1) with

$$\beta_W = \frac{0.06238\, m^{(m-1)/4}}{4^{(m-5)/4}\Gamma[(m-1)/4]}[1 + 0.7458(m+2)^{-1.057}], \tag{5}$$

$$T_p = T_{H1/3}/[1 - 0.283(m-1.5)^{-0.684}], \tag{6}$$

$$T_p = \bar{T}/[1 - 1.295(m-0.5)^{-1.072}]. \tag{7}$$

FORMULA II: Modified JONSWAP-type of Eq. (2) with

$$\beta_J = \frac{0.06238}{0.230 + 0.0336 - 0.185(1.9+\gamma)^{-1}}[1.094 - 0.01915 \ln \gamma], \tag{8}$$

$$T_p = T_{H1/3}/[1 - 0.132(\gamma + 0.2)^{-0.559}], \tag{9}$$

$$T_p = \bar{T}/[1 - 0.532(\gamma + 2.5)^{-0.569}]. \tag{10}$$

The portions of the fractions in the right-hand sides of Eqs. (5) and (8) represent the constants determined by the relation $H_{1/3} = 4.004\,\sigma_\eta$, while those within the brackets provide the corrections for the deviation of $H_{1/3}$ from the above relation or the value $[4.004\,\sigma_\eta/H_{1/3}]^2$. The adequacy of Eqs. (5) through (10) can be checked easily by comparing the predictions by them with the data listed in Tables 1 and 2.

Although the formulas I and II should yield the same values of constants for the cases of $m = 5$ and $\gamma = 1$, there exists a small amount of difference because of fitting error. By neglecting such a difference, the spectrum for $m = 5$ and $\gamma = 1$ is written as

$$S(f) = 0.205\,H_{1/3}^2 T_{H1/3}^{-4} f^{-5} \exp[-0.75(T_{H1/3}f)^{-4}], \tag{11}$$

or

$$S(f) = 0.103\,H_{1/3}^2 \bar{T}^{-4} f^{-5} \exp[-0.38(\bar{T}f)^{-4}]. \tag{12}$$

Equation (11) is the alternative to the commonly used Bretschneider-Mitsuyasu formula of the following:

$$S(f) = 0.257\,H_{1/3}^2 T_{H1/3}^{-4} f^{-5} \exp[-1.03(T_{H1/3}f)^{-4}]. \tag{13}$$

This equation was based on the relation $T_p = 1.05\,T_{H1/3}$ which was introduced by Mitsuyasu (1970). This relation seems to reflect the influence of the presence of the low frequency components in almost all wave records in the sea. There is also a possibility that the data by Mitsuyasu may have represented the spectrum of wind waves under the action of strong winds in relatively short fetch which had the spectral peak sharper than that by Eq. (13).

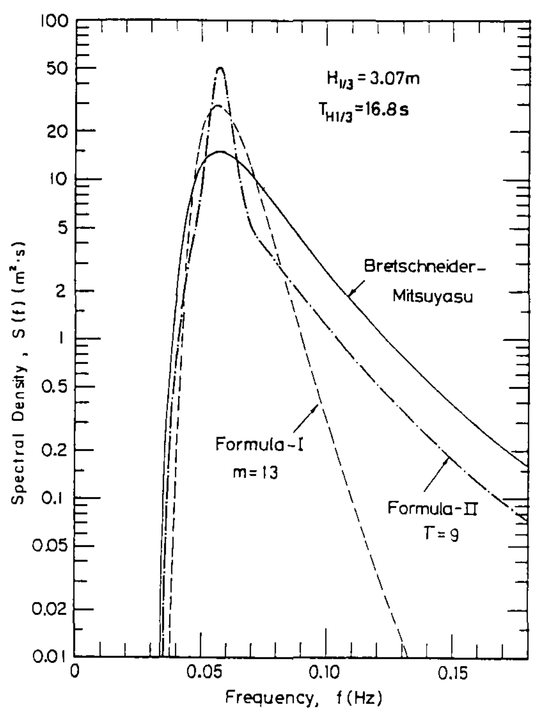

Fig. 1 Comparison of model spectra.

Table 3 Proportionality coefficient α of the standard deviation (S.D.) and the coefficient of variation (C.V.) of various statistical parameters of Wallops-type spectrum

Parameter	(Type)	$m = 3$	$m = 4$	$m = 5$	$m = 6$	$m = 8$	$m = 10$	$m = 14$	$m = 20$	Caldera Port
$\sqrt{\beta_1}$	(S.D.)	0.93	0.82	0.72	0.62	0.44	0.32	0.16	0.08	0.95
β_2	(S.D.)	2.29	2.44	2.57	2.69	2.89	3.05	3.30	3.49	3.52
β_3	(S.D.)	0.88	0.82	0.77	0.71	0.55	0.40	0.21	0.09	1.16
[C.V. (H_{max})]*	(C.V.)	0.85*	0.88*	0.90*	0.92*	0.93*	0.95*	0.97*	1.01*	0.98*
σ_η	(C.V.)	0.49	0.53	0.55	0.58	0.62	0.65	0.71	0.77	0.75
$H_{1/10}$	(C.V.)	0.64	0.67	0.70	0.72	0.77	0.81	0.87	0.94	0.79
$H_{1/3}$	(C.V.)	0.57	0.58	0.60	0.61	0.65	0.69	0.74	0.80	0.82
$\bar{H}$	(C.V.)	0.61	0.63	0.64	0.65	0.67	0.70	0.75	0.81	0.97
σ_H	(C.V.)	0.74	0.77	0.79	0.83	0.89	0.93	1.01	1.09	1.03
$H_{1/10}/\sigma_\eta$	(C.V.)	0.37	0.38	0.40	0.41	0.43	0.45	0.49	0.53	0.49
$H_{1/3}/\sigma_\eta$	(C.V.)	0.22	0.19	0.17	0.16	0.16	0.17	0.18	0.20	0.18
$\bar{H}/\sigma_\eta$	(C.V.)	0.33	0.32	0.30	0.28	0.26	0.25	0.24	0.24	0.42
$H_{1/10}/H_{1/3}$	(C.V.)	0.34	0.35	0.36	0.36	0.38	0.39	0.42	0.44	0.41
$H_{1/3}/\bar{H}$	(C.V.)	0.30	0.32	0.32	0.32	0.33	0.34	0.36	0.38	0.50
$T_{H1/10}$	(C.V.)	0.64	0.54	0.48	0.43	0.36	0.31	0.26	0.22	0.21
$T_{H1/3}$	(C.V.)	0.49	0.40	0.35	0.31	0.27	0.24	0.20	0.17	0.19
$\bar{T}$	(C.V.)	0.51	0.44	0.40	0.36	0.31	0.28	0.25	0.22	0.44
σ_T	(C.V.)	0.66	0.63	0.65	0.69	0.72	0.74	0.81	0.88	1.05
$T_{H1/10}/T_{H1/3}$	(C.V.)	0.57	0.48	0.43	0.38	0.32	0.28	0.22	0.18	0.18
$T_{H1/3}/\bar{T}$	(C.V.)	0.40	0.38	0.37	0.34	0.31	0.28	0.25	0.21	0.51

Note: The figures superscribed with * refer to the ratio of the observed value to the theoretical prediction by the Rayleigh distribution.

Table 4 Proportionality coefficient α of the standard deviation (S.D.) and the coefficient of variation (C.V.) of various statistical parameters of JONSWAP-type spectrum

Parameter	(Type)	$\gamma = 1.5$	$\gamma = 2$	$\gamma = 3.3$	$\gamma = 5$	$\gamma = 7$	$\gamma = 10$	$\gamma = 14$	$\gamma = 20$	Caldera Port
$\sqrt{\beta_1}$	(S.D.)	0.69	0.66	0.62	0.57	0.52	0.47	0.42	0.38	0.95
β_2	(S.D.)	2.62	2.61	2.77	2.95	2.96	3.27	3.36	3.68	3.52
β_3	(S.D.)	0.77	0.76	0.75	0.72	0.71	0.68	0.64	0.60	1.16
{C.V. (H_{max})}*	(C.V.)	0.91*	0.90*	0.94*	0.96*	0.98*	1.02*	1.04*	1.09*	0.98*
σ_η	(C.V.)	0.58	0.61	0.68	0.74	0.80	0.87	0.94	1.00	0.75
$H_{1/10}$	(C.V.)	0.73	0.75	0.83	0.89	0.95	1.03	1.09	1.17	0.79
$H_{1/3}$	(C.V.)	0.62	0.65	0.72	0.78	0.84	0.91	0.97	1.04	0.82
$\bar{H}$	(C.V.)	0.67	0.71	0.77	0.83	0.89	0.96	1.03	1.08	0.97
σ_H	(C.V.)	0.82	0.84	0.92	0.99	1.04	1.13	1.21	1.31	1.03
$H_{1/10}/\sigma_\eta$	(C.V.)	0.40	0.39	0.42	0.44	0.46	0.50	0.53	0.57	0.49
$H_{1/3}/\sigma_\eta$	(C.V.)	0.17	0.17	0.16	0.16	0.17	0.17	0.18	0.19	0.18
$\bar{H}/\sigma_\eta$	(C.V.)	0.31	0.31	0.32	0.33	0.33	0.34	0.36	0.36	0.42
$H_{1/10}/H_{1/3}$	(C.V.)	0.36	0.36	0.39	0.41	0.41	0.44	0.46	0.49	0.41
$H_{1/3}/\bar{H}$	(C.V.)	0.32	0.33	0.35	0.37	0.39	0.41	0.44	0.46	0.50
$T_{H1/10}$	(C.V.)	0.44	0.40	0.35	0.30	0.26	0.24	0.20	0.19	0.21
$T_{H1/3}$	(C.V.)	0.32	0.30	0.26	0.23	0.20	0.17	0.15	0.14	0.19
$\bar{T}$	(C.V.)	0.40	0.41	0.40	0.39	0.39	0.37	0.35	0.32	0.44
σ_T	(C.V.)	0.64	0.63	0.66	0.72	0.82	0.97	1.14	1.32	1.05
$T_{H1/10}/T_{H1/3}$	(C.V.)	0.40	0.37	0.32	0.29	0.26	0.22	0.20	0.17	0.18
$T_{H1/3}/\bar{T}$	(C.V.)	0.36	0.37	0.36	0.36	0.36	0.35	0.34	0.32	0.51

Note: The figures superscribed with * refer to the ratio of the observed values to the theoretical prediction by the Rayleigh distribution.

Figure 1 presents a comparison of spectral shapes by the formulas I, II and the Bretschneider-Mitsuyasu spectra. The spectral shape parameters are arbitrarily chosen at m = 13 and γ= 9. The formula II or the modified JONSWAP-type spectrum has a sharply enhanced peak compared with that of the Bretschneider-Mitsuyasu spectrum. The formula I or the modified Wallops-type spectrum is characterized by a rapid decrease of spectral density at the high frequency range, but its peak is not as sharp as that of the formula II spectrum.

In laboratory simulation of ocean waves, the input data for wave spectrum is often limited to the significant wave height and some representative wave period such as $T_{H1/3}$, $\bar{T}$, or T_p, because reliable spectral data for the design condition is not available in many cases. Under such circumstances, the new formulas I and II will serve for the need of spectral specification in laboratory tests. The applicability of the formulas I and II for mechanically generated irregular waves has been confirmed by the data in the author's laboratory.

V. STANDARD DEVIATIONS OF SEA STATE PARAMETERS

The standard deviations of sea state parameters generally decreases as the length of a wave record increases. The rate of decrease is inversely proportional to the square root of the number of zero-upcrossing or zero-downcrossing waves per record except for H_{max} and $T_{H,max}$. This inverse proportionality can be proven for σ_η by Tucker's theory (1957) and for the mean wave period $T_{0,2}$ by Cavanié's theory (1979). The author has demonstrated the inverse proportionality for several height and period parameters by numerical simulation (Goda 1977).

With the knowledge of the above, the data of the standard deviations of various sea state parameters obtained by the present study are expressed in the following form:

$$\sigma(x) = \alpha N_0^{-1/2}, \quad \text{or} \quad \text{C.V.}(x) = \alpha N_0^{-1/2}, \tag{14}$$

where x stands for a sea state parameter, α denotes the proportionality coefficient, and C.V. refers to the coefficient of variation. The standard deviation is used for the surface elevation parameters $\sqrt{\beta_1}$, β_2, and β_3, while the coefficient of variation is applied for the rest of parameters. Tables 3 and 4 list the results of the proportionality coefficient α for various parameters, which is evaluated as the average of the estimates for simulated wave profiles with the data points 512 to 4096. The following is some comments on the results of Tables 3 and 4.

Parameters of Surface Elevation

The skewness $\sqrt{\beta_1}$ and the kurtosis β_2 have the theoretical mean values of 0 and 3, respectively. The numerical data have confirmed these theoretical values. The coefficient α for the skewness $\sqrt{\beta_1}$ decreases as the wave spectrum becomes sharply peaked, while the coefficient α for the kurtosis β_2 increases. A slight deviation from the relation of Eq. (14) is observed for β_2 for waves with sharply peaked spectra; the rate of decrease of $\sigma(\beta_2)$ with N_0 is slower than Eq. (14).

The parameter β_3 is a new parameter called the wave atiltness introduced by the author (1985b) with the definition of

$$\beta_3 = \frac{1}{N-1}\sum_{i=1}^{N-1}(\dot{\eta}_i - \bar{\dot{\eta}})^3 \Bigg/ \left\{\frac{1}{N-1}\sum_{i=1}^{N-1}(\dot{\eta}_i - \bar{\dot{\eta}})^2\right\}^{3/2}, \tag{15}$$

where N denotes the number of data points and the superscript "dot" denotes the time derivative. The atiltness is a measure of wave asymmetry in the horizontal direction. It is zero when a wave profile is statistically symmetric, and positive when a wave profile is tilted forward with a rapid rise and a gradual fall. The atiltness β_3 takes a large positive value in the water area from the outer edge toward the middle of the surf zone, where the upcrossing definition yields larger values of period parameters than the downcrossing definition (Goda, 1986). The coefficient α for the atiltness β_3 shows a tendency similar with that for the skewness $\sqrt{\beta_1}$.

Maximum Wave Height and Period

The theory of the Rayleigh distribution predicts the following value for C.V.($H_{\max}$) [e.g., Goda, 1985a, p. 229]:

$$\mathrm{C.V.}(H_{\max}) = \frac{\pi}{2\sqrt{6}\ln N_0} \Big/ \left(1 + \frac{\zeta}{2\ln N_0}\right). \tag{16}$$

Because Eq. (14) is not applicable for C.V.($H_{\max}$), the ratio of the value obtained by simulation to the prediction by Eq. (16) is listed in Tables 3 and 4. The difference between the simulation and the theory is generally small, although C.V.($H_{\max}$) tends to become smaller than the prediction as the spectral peak becomes broad. As for the coefficient of variation of $T_{H,\max}$, Fig. 2 is prepared on the basis of simulation data, because there exists no theory available.

Wave Height Parameter

The wave height parameters indicate uniform increases in their coefficients of variation as the wave spectrum becomes sharply peaked. It should be noted that the coefficient of variation of $H_{1/3}$ is smaller than that of $\bar{H}$. This means that $H_{1/3}$ has a smaller sampling error than $\bar{H}$ and thus $H_{1/3}$ is a more reliable parameter than $\bar{H}$.

Wave Height Ratio

The ratios between various wave height parameters are not so sensitive to the change in spectral shape. Especially the ratio $H_{1/3}/\sigma_\eta$ has almost a constant value of α over the various spectral shapes under investigation. Although the tendency of variation in C.V.($\bar{H}/\sigma_\eta$) with respect to the sharpening of spectral peak is different between the cases of the Wallops-type and the JONSWAP-type spectra, its reason is not clarified at this stage.

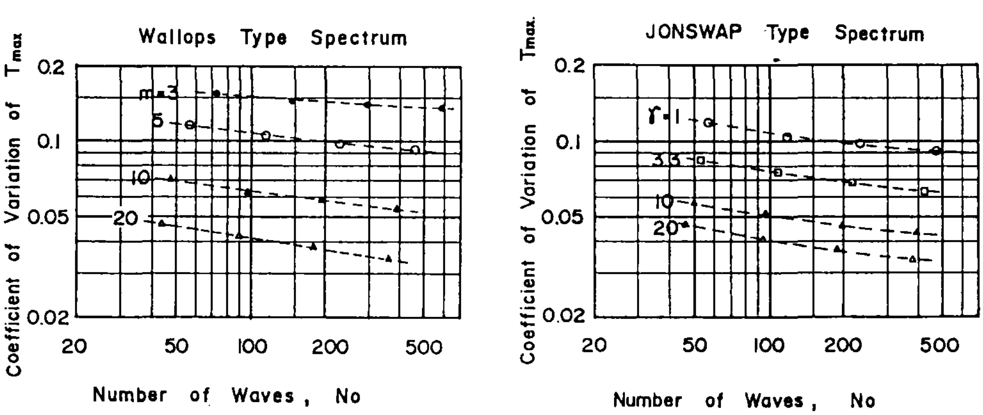

Fig. 2 Coefficient of variation of $T_{H,\max}$.

Wave Period Parameter and Period Ratio

The wave period parameters and their mutual ratios indicate uniform decreases in their coefficients of variation as the wave spectrum becomes sharply peaked. The only exception is the parameter σ_T which shows an increase in its coefficient of variation with sharpening of spectral peak.

Correlation Coefficient

A correlation coefficient between two statistical variables has the following variance [e.g., Kendall and Stuart 1969, p. 236]:

$$\mathrm{Var}[r] = (1 - r^2)^2/n, \qquad (17)$$

where n is the number of samples and r is the correlation coefficient in the ensemble. In the cases of r_{HT} and r_{HH}, n is taken as N_0 and $N_0 - 1$, respectively. The standard deviations of r_{HT} and r_{HH} predicted by Eq. (17) are slightly less than the observations in the simulation, but the differences are small.

VI. VARIABILITY OF SEA STATE PARAMETERS IN FIELD DATA

Verification of statistical variability of sea state parameters in the field is rather difficult, because no one can answer with confidence to the question whether the same sea state condition is continuing or not. One of rare occasions is the case of wave registration of long-travelled swell in May 1981 at Caldera Port in Costa Rica, Central America, reported by the author (1983a). The swell travelled over nearly 7000 km, and its intensity attenuated only gradually. Figure 3 shows the variations of swell heights, periods, and correlation coefficients over 14 hours, which were analyzed for every 30 minutes from a long continuous record. Figure 4 exhibits the average frequency spectrum of this swell. The second peak at the frequency 0.11 Hz is due to the secondary interaction between spectral components (Goda 1983a, b).

The sea state parameters analyzed from 27 consecutive records were processed for the statistical examination. The gradual decrease in wave heights and periods is owing to the velocity dispersion of swell. A linear regression line was applied for the data of each sea state parameter, and the ratio of each data to the value on the respective regression line was employed for the statistical analysis. The proportionality coefficient α was calculated for each parameter by applying Eq. (14). The number of wave N_0 varied between 110 and 129, and the average value 118.6 was used to calculate α. The results are listed in the right-hand columns of Tables 3 and 4.

Compared with the data by the simulation study, most of the swell data of Caldera Port approximately fit to the case of the Wallops-type spectrum with m= 10 to 20 or the case of the JONSWAP-type spectrum with γ= 5 to 14. Exceptions are the cases of the skewness and atiltness of the surface elevation, which show larger deviations than the simulation data. These deviations are considered to be owing to the strong nonlinearity effect in shallow water (about 17 m deep at the site of wave sensor). The parameters related with $\bar{H}$ and $\bar{T}$ are not well fitted to the simulation data, probably because the Caldera swell data contain some locally-generated wind waves.

The dash-dot line in Fig. 4 represents the model spectrum by the formula II with γ= 9; a relatively good agreement is seen between the observed and model spectra. Because other spectral data also exhibited the characteristics similar with the JONSWAP-type spectra with γ= 8 to 9 (Goda 1983a), the statistical variability data of Caldera Port confirms the validity of the present simulation study.

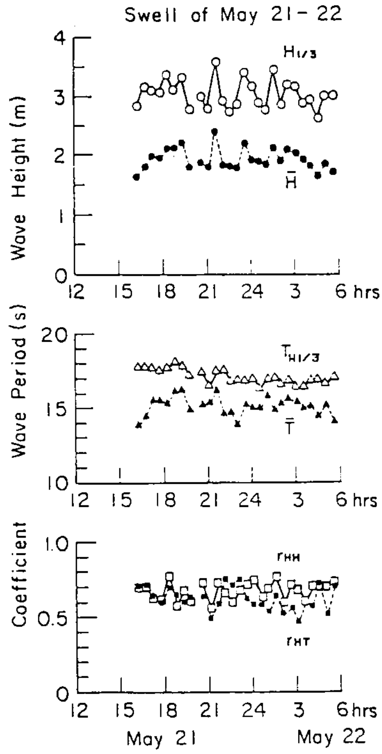

Fig. 3 Time variation of sea state parameter of swell at Caldera Port.

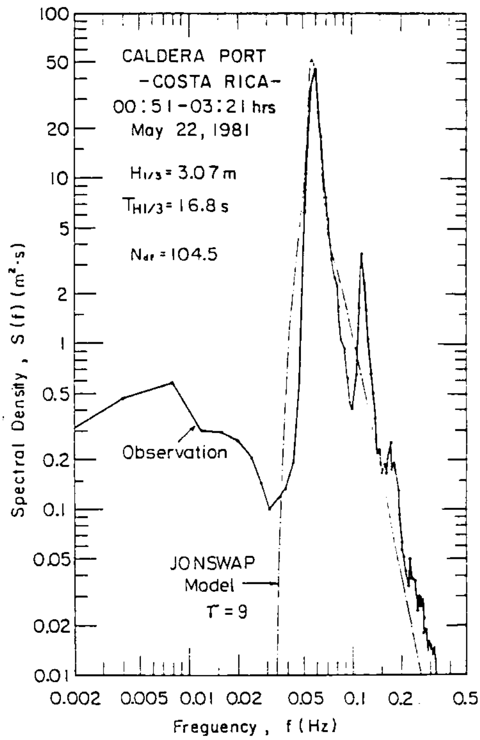

Fig. 4 Example of average swell spectrum compared with JONSWAP-type model spectrum.

Comparison was also made between the observed values of several wave height and period ratios with the simulation data listed in Tables 1 and 2. The ratios $H_{max}/H_{1/3}$ and $H_{1/10}/H_{1/3}$ of Caldera Port data showed the mean values smaller than the simulation data, while the mean value of the ratio $H_{1/3}/\bar{H}$ was almost the same with the simulation data. The mean values of the ratios $T_{H,max}/T_{H1/3}$ and $T_{H1/10}/T_{H1/3}$ were quite close to 1, while that of $T_{H1/3}/\bar{T}$ was 1.15. The result of the above period ratio in addition to the foregoing result of statistical variability data suggests that the JONSWAP-type spectrum with γ= 7 to 10 is a more appropriate model for the long-travelled swell at Caldera Port than the Wallops-type spectrum. The high value of the correlation coefficient r_{HT} (mean of 0.62) supports the above conclusion.

VII. SUMMARY

The findings obtained by the present simulation study are summarized as follows:

1) The mean values of various wave height and period parameters are given for the variety of the Wallops-type and the JONSWAP-type spectra. These values will serve as the basis of reference to the field data analysis and the theoretical development of zero-upcrossing or zero-downcrossing height and period statistics.

2) The modified forms of the Wallops and the JONSWAP spectra are proposed with the input data of the significant wave height and a representative period parameter. The formula will serve for the need of spectral specification in laboratory tests of irregular waves.

3) The standard deviations and the coefficients of variation of various sea state parameters are evaluated as the function of spectral shapes. The information can be used to estimate the magnitude of the standard error of any sea state parameter obtained from a wave record.
4) The statistical properties of the swell travelled over 7000 km are in agreement with those of the JONSWAP-type spectral waves with $\gamma = 7$ to 10. The agreement confirms the validity of the findings by the present study.

REFERENCES

Cavanié, A., A. Arhan, and R. Ezraty (1976): A statistical relationship between individual heights and periods of storm waves, Proc. BOSS '76, Vol. II, pp. 354–360.
Cavanié, A.G. (1979): Evaluation of the standard error in the estimation of mean and significant wave heights as well as mean period from records of finite length, Proc. Int. Conf. Sea Climatology, pp. 73–88.
Goda, Y. (1977): Numerical experiments on statistical variability of ocean waves, Rept. Port and Harbour Res. Inst., Vol. 16, No. 2, pp. 3–26.
Goda, Y. (1978): The observed joint distribution of periods and heights of sea waves, Proc. 16th Int. Conf. Coastal Eng., pp. 227–246.
Goda, Y. (1983a): Analysis of wave grouping and spectra of long-travelled swell, Rept. Port and Harbour Res. Inst., Vol. 22, No. 1, pp. 3–41.
Goda, Y. (1983b): A unified nonlinearity parameter of water waves, Rept. Port and Harbour Res. Inst., Vol. 22, No. 3, pp. 3–30.
Goda, Y. (1985a): Random Seas and Design of Maritime Structures, Univ. Tokyo Press, Tokyo, 323p.
Goda, Y. (1985b): Numerical examination of several statistical parameters of sea waves, Rept. Port and Harbour Res. Inst., Vol. 24, No. 4, pp. 65–102 (in Japanese).
Goda, Y. (1986): Effect of wave tilting on zero-crossing wave heights and periods, Coastal Engg. in Japan, JSCE, pp. 79–90.
Goda, Y. (1987): Statistical variability of sea state parameters as a function of wave spectrum, Proc. IAHR Seminar on Wave Analysis and Generation in Laboratory Basins, September 1987, National Research Council of Canada, pp. 237–248.
Hasselmann, K. et al. (1973): Measurements of wind-wave growth and swell decay during the Joint North Sea Wave Project (JONSWAP), Deutsche Hydr. Zeit, Reihe A (8), No. 12.
Huang, N.E. et al. (1981): A unified two-parameter wave spectral model for a general sea state, J. Fluid Mech., Vol. 112, pp. 203–224.
Kendall, M.G. and A. Stuart (1969): The Advanced Theory of Statistics, Vol. 1 (3rd Ed.), Griffin, London.
Longuet-Higgins, M.S. (1952): On the statistical distributions of the heights of sea waves, J. Marine Res., Vol. IX, No. 3, pp. 245–266.
Longuet-Higgins, M.S. (1975): on the joint distribution of the periods and amplitudes of sea waves, J. Geophysical Res., Vol. 80, No. 18, pp. 2688–2694.
Longuet-Higgins, M.S. (1983): On the joint distribution of wave periods and amplitudes in a random field, Proc. Roy. Soc. London, Ser. A, Vol. 389, pp. 241–258.
Mitsuyasu, H. (1970): On the growth of spectrum of wind-generated waves (2)—spectral shape of wind waves at finite fetch—, Proc. 17th Japanese Conf. Coastal Eng., pp. 1–7 (in Japanese).
Tayfun, M.A. (1983): Effects of spectrum band width on the distribution of wave heights and periods, Ocean Eng., Vol. 10, No. 2, pp. 107–118.
Tucker, M.J. (1957): The analysis of finite-length records of fluctuating signals, British Jour. Applied Physics, Vol. 8, April, pp. 3–41.

(Received Mar. 24, 1988; revised May 29, 1988)